

# SCATTERING IN THE OCEAN

L.J. Hamilton (editor), S. Anstee, P.B. Chapple, M.V. Hall and P.J. Mulhearn

Maritime Operations Division,  
Defence Science & Technology Organisation (DSTO),  
P.O. Box 44, Pyrmont, NSW 2009, Australia

**ABSTRACT** Acoustic scattering in the ocean can arise naturally from interactions of sound with suspended particles, volume inhomogeneities, bubbles, the moving random sea surface, the seabed, and organisms, either in resonant or nonresonant processes. Measurements of backscatter stimulated via these processes by active sonar associated with these phenomena generated by active sonar devices are becoming increasingly useful as remote sensing tools in highly diverse applications. These include assessments of fish stocks and fish migration, seabed and habitat characterization, inferences of turbidity, measurements of waves and currents, and detection of objects. Some of these applications are broadly described, together with the physical scattering mechanisms involved.

## 1. INTRODUCTION

Scattering processes in the from the ocean environment ocean causes reverberation, a major part of the unwanted background noise level that hinders military active operations of active sonars seeking to detect sound scattered by ships, submarines, and mines. Military sonar designs have previously sought to suppress environmental scattering to enhance their target-seeking ability. However, environmentally backscattered<sup>1</sup> sound Without backscattering in particular, which is that portion of the scattering that propagates directly back to the position of the transmitter, there would be no reverberation and sonar detection ranges would be vastly increased. So then, what good is marine acoustic scattering? Why should it be of interest? The answer is that from traditionally being a major handicap in marine sonic applications, backscatter now finds a surprisingly large number of applications in underwater acoustics. It is essentially used as a means of remote sensing, and as such can be used to quickly examine large oceanic volumes, or large areas of the air/sea or sea/bottom interfaces. Optical devices experience high attenuation, but direct sound transmission and acoustic backscatter can be used to probe oceanic processes over a very wide frequency range (Hz to MHz). Many interesting physical problems arise in marine acoustic scattering, since it involves interactions with physical, chemical, biological, geometrical, and geological properties of the environment. One of the more interesting applications can be found in sidescan sonars, which provide high resolution-high-resolution pictures of the seabed similar to video imagery. Other backscatter devices can infer concentrations of suspended solids at high levels where the usual optical measures are defeated.

Scattering is a function of frequency, being stronger for higher frequency components of a signal, and also of the size, compressibility, shape, and density of the scatterers, which can be discrete bodies (suspended particles), or roughness elements on a continuous surface. Scattering is a reradiation of incident acoustic energy. At low frequencies (wavelength  $\lambda$  much greater than the scatterer size) scattering is omnidirectional, while at high frequencies the scattering becomes directional (and the particle will cast a shadow).

Ocean water is turbid for light, but transparent for sound, because suspended particles are generally 1 to 10 microns in size, which makes them larger than optical wavelengths, but

smaller than acoustical wavelengths (a 1-MHz sound wave has a wavelength of 1.5 mm). The optical cross section of a typical particle is similar to its geometrical cross-section, but its acoustic cross section is much smaller than its geometrical cross-section [6].

Optical devices experience high attenuation, but sound and acoustic backscatter can be used to probe oceanic processes over a very wide frequency range (Hz to MHz). Many interesting physical problems arise in marine acoustical scattering, involving as it does interactions with physical, chemical, biological, geometrical, and geological properties of the environment.

## 2. SCATTERING THEORY AND HIGH FREQUENCY SONARS (S. S. Anstee)

High-frequency sonars are the acoustic equivalent of vision systems, and work in much the same way. If something radiates sound, a sonar can use the phase and amplitude information in the radiated waves to estimate the location and nature of the source. However, most of the underwater environment does not spontaneously radiate sound, so many sonars rely on scattered sound, that is, sound bounced from objects and interfaces from irregularities in the environment. Optical vision systems can often rely on intense external sources of radiation – the sun, room lighting and so on – to provide a radiation source. Natural sources of acoustic radiation are much weaker, although the technology for passive sonars relying on scattering of environmental noise, so called “acoustic daylight”, is in development [26]. Most sonars relying on scattered sound are active, that is, they provide their own intense acoustic radiation source, most often adjacent to the receiver. The sound they emit is usually pulsed and coherent, more like a laser beam than a torch, with the energy centred on a relatively narrow band of frequencies<sup>2</sup>.

When there is no change in sound speed, a sound wave propagates away from the source indefinitely, never returning.

<sup>1</sup> Backscattered sound is that part of the total scattered sound that goes back towards the source.

<sup>2</sup> Some active sonars are “broad-band”, with bandwidths of one or more octaves. Such sonars emit pulses that can appear incoherent or “noisy”, but knowledge of the exact waveform allows the sonar processor to select only echoes with exactly matching waveforms, thereby greatly increasing the signal to noise ratio.

However, when a travelling wave encounters an abrupt change or interface between two media with different physical properties, only part of the wave is transmitted across the interface, with the rest returning to the original medium. The phases and amplitudes of the transmitted and returned waves now contain additional information about the interface they encountered, encoded as phase and amplitude changes.

The field after the wave hits an interface can be expressed as

$$p(\mathbf{r}, t) = p_{in}(\mathbf{r}, t) + p_s(\mathbf{r}, t) \quad (1)$$

the sum of the original, *incident* field and a new *scattered* field. Scattering is a reradiation of incident acoustic energy. *Reflection* is a special case of scattering where the scattered field retains most of the information in the incident field. If the interface is completely flat, the reflected field is (to within a scale factor) just the incident field that would have originated from a source placed at the reflected position of the true source, multiplied by a phase factor. *Scattering* is usually taken to mean the more general case where most of the original phase information is lost and the bulk of the information carried by the scattered field describes the interface it scattered from.

Scattering is a function of frequency, being stronger for higher frequency components of a signal, and also of the size, compressibility, shape, and density of the scatterer, which can be one or more discrete objects, or roughness elements on a continuous surface. At low frequencies (wavelength  $\lambda$  much greater than scatterer size, the Rayleigh criterion) scattering is omnidirectional, while at high frequencies the scattering becomes directional (and the object will cast a shadow). In general ocean water is turbid for light, but transparent for sound, even at several hundreds of kHz, because suspended particles (grains of clay) are typically 1 to 10 microns in size, which makes them larger than optical wavelengths, but smaller than acoustic wavelengths (a 1-MHz sound wave has a wavelength of 1.5 mm). The optical cross section of a typical particle (but not a bubble) is similar to its geometrical cross-section, but its acoustic cross section is much smaller than its geometrical cross-section [6]. Acoustic backscattering can therefore carry more energy over longer distances than optical wavelengths.

#### Discrete scatterers

The simplest scattering object is a sphere of gas immersed in a liquid, e.g., an air bubble in water. When a mono-frequency plane wave with frequency  $\omega$  radians per second travelling through the liquid and striking the sphere continues on, but the total field thereafter now includes a second, scattered field,  $p_s$ . For Rayleigh scattering the scattered pressure takes the form

$$p_s(\mathbf{r}, t) = a_0 k^2 \frac{e^{i(kr - \omega t)}}{r} \quad (2)$$

Here,  $r$  is the radial distance;  $k = 2\pi/\lambda$  is the wavenumber; and is  $a_0$  complex constant. This is simply a travelling wave radiating outward from the scatterer, which functions like an elementary source. The wave contains no information about the source of the incident radiation, except for amplitude. A very

small liquid or solid sphere also has this form of scattered pressure, but with an additional dipole term that preferentially forward- and back-scatters sound along the direction of propagation. An arbitrarily shaped small object also generates the same form of scattered field as a small sphere. Hence, when a sonar pings at water containing suspended sediments and plankton, each particle acts as a spherical scatterer and some of the energy is backscattered to the sonar as *volume reverberation*. Although the incoming sound is coherent, the particles are randomly distributed and the backscattered sound is an *incoherent* sum of waves with random phases and amplitudes.

#### Larger objects and surfaces

Scattering by larger objects and surfaces is more complicated, with a combination of reflection and random scattering contributing to the total pressure field. The field scattered by an arbitrary closed surface can be entirely described by the pressures and pressure gradients at the surface. The surface can be considered as a collection of elemental sources and dipoles, each radiating in all directions. When the surface is perfectly flat, the individual contributions all add in phase (coherently), and the form of the scattered pressure is similar to the form of becomes the same as the incident pressure times a constant, but appearing to come from a different source – “specular” scattering.

Both the seabed and sea surface can be approximated as flat surfaces perturbed by roughness, and the scattered field can then be predicted. However, the resulting equation is generally difficult to solve.

If we assume that each surface element acts like an infinite plane and ignore any interactions between elements, then  $p(\mathbf{r}') = (1+R)p_{in}(\mathbf{r}')$  and,  $\nabla' p(\mathbf{r}') = (1-R)\nabla' p_{in}(\mathbf{r}')$ , where  $R$  is the plane-wave reflection coefficient the surface would have if it were uniform and flat. Then the solution for the scattered pressure equation collapses to a function of the incident pressure and is easy to evaluate. This is the *Kirchhoff* or *physical acoustics* approximation. Experimentally it is a good fit for backscatter when the sonar looks steeply down at the seabed or up at the sea surface, and for forward scatter, as long as the surface is not too rough. It is a poor approximation when the sound approaches the surface from a shallow angle, but in such cases, another approximation, the *small roughness* approximation, may be used. In this approximation, seabed roughness is treated as a vertical perturbation away from a flat surface and the surface pressure is perturbed by an amount  $p_s(\mathbf{r}') \approx -h(\partial p_{in}/\partial z + \partial p_s^{(0)}/\partial z)$ , where  $z$  is vertical direction,  $h$  the vertical roughness scale and the pressure field that would be scattered from a perfectly flat surface. It turns out that the first-order *coherent* field is zero – the roughness makes no difference to the energy reflected from the underlying flat surface, but the first order *diffuse* or *incoherent* field is non-zero. The diffuse field is sensitive to the proportion of points on the surface that happen to be correctly separated to scatter sound at the observing direction, as though the surface were a random ensemble of Bragg diffraction gratings. In between steep and shallow incident angles, it is possible to interpolate between the small roughness and Kirchhoff regimes, or use

other, more general approximations. In situations of extreme roughness, all of these approximations break down and an empirical approach is taken.

### 3. ACOUSTICAL SEABED IMAGING

(P.B. Chapple)

Acoustic backscatter from the seabed can be used to image the seabed, enabling active sonar systems to provide valuable information about seabed properties. Acoustics is particularly important in this role, because ocean waters are usually too deep and turbid for optical imaging to be effective. Information obtainable includes bathymetry (depth), seabed hardness, clutter, slope and the presence of objects on the seafloor. At frequencies less than about 50 kHz, significant energy can penetrate the seabed, particularly for soft sediments, and some sub-bottom information can be obtained using suitably designed systems. At higher frequencies, there is very little seabed penetration, and information obtained from seabed backscatter essentially indicates the properties of the seabed surface. Using frequencies as high as 500 kHz, it is possible to image the seabed with 10 to 20 cm horizontal resolution, although range is often limited to about 100 m.

The most popular method of acoustically imaging the seabed is using sidescan sonar (Figure 1). Acoustic energy is emitted from either side of a moving vessel, or from a towfish pulled by the vessel, from horizontal linear arrays of transducers on the port and starboard sides which point slightly downwards. The beamwidth is narrow in the along-track direction, but broad in elevation or across-track direction, enabling a thin strip or narrow swathe to be ensonified perpendicular to the array with each sonar ping (Figure 1). Backscattered energy from the seabed is used to build an image of the seabed, strip by strip, as the vessel moves along. The timing of the return signal from each acoustic pulse is used for estimating the range of the patch of seabed contributing to the signal. A "waterfall" display of the seabed is formed as the vessel moves along (Figure 2(a)).

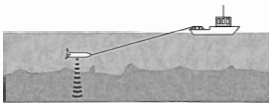


Figure 1: (a) Towed sidescan sonar.

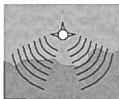


Figure 1: (b) End view of towfish

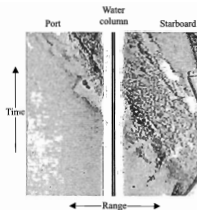


Figure 2: (a) Waterfall image, that scrolls downwards during data acquisition (from the Klein 5500 sidescan sonar). Smooth seabed on the lower left is disrupted by the rough surface of the Sydney Harbour tunnel.



Figure 2: (b) Mosaic image of the seabed of Sydney Cove, including Circular Quay wharves and the rough surface above the Harbour Tunnel.

The depth of a sloping seabed cannot be reliably estimated from sidescan sonar. A flat-bottom assumption is made in order to estimate the location of each part of the imaged seabed, which is calculated from a combination of range, estimated position of the towfish relative to the towing vessel and the differential GPS position acquired at the boat. Utilising this information, a mosaic image of the seabed can be formed (Figure 2(b)) from numerous boat tracks.

The texture of sidescan sonar images can be used to characterise the seabed, by segmentation into regions with different textural statistics, indicating the presence of mud or sand, scattered rock and other bottom types. Several difficulties arise in this approach: (i) The appearance of the seabed in a sidescan image depends on the distance from the nadir. There is generally poor horizontal resolution in the nadir

region. (ii) The appearance of features such as sand waves depends strongly on the direction of ensonification. (iii) Seabed slope significantly affects the appearance of sidescan imagery, complicating attempts to determine seabed type.

Multibeam echosounder systems allow seabed imaging with bathymetric information. While the feature detection capabilities are not usually as good as for sidescan sonar, some modern systems such as the Reson 8125 have very high spatial resolution. Bathymetric relief images can be segmented to delineate different broad-scale texture regions, with the seabed characterisation independent of the direction of ensonification. Further seabed information can be obtained by measuring the backscatter magnitude as a function of the angle of incidence of the acoustic wave on the seabed.

#### 4. SEABED PROPERTIES MODELLING AND INVERSION TECHNIQUES (P.J. Mulhearn)

The shapes and energies of echoes received by echosounders depend on bottom acoustic hardness and roughness. The first part of the echo shape is a peak dominantly from specular return, and the second part is a decaying tail principally from incoherent backscatter contributions. Rougher sediment surfaces provide more backscattered energy than smoother surfaces (which simply reflect the energy away from the direction of the transducer), so their echoes are expected to have lower peaks and longer tails than smoother surfaces of the same composition. Echo shape is also affected by sub-bottom volume reverberation including contributions from gas bubbles, and echosounder characteristics such as frequency, ping length, ping shape, and beam width.

A number of acoustic seabed classification systems are commercially available which can be used to estimate seabed properties from echo characteristics [14] using one of two empirical methods: (i) echo statistics are obtained at a number of sites with known seabed type, to calibrate the system. The whole area is then surveyed, and the seabed classified as belonging to one of these types; or (ii) an area is surveyed and the echoes are grouped by some statistical technique into a number of classes, which are subsequently ground-truthed. At times the first approach may reveal seabed types for which calibrations were not obtained, so that some post calibration is required.

The oldest commercial system is RoxAnn, which uses the first and second echoes from the seabed [4,16]. The first echo simply travels from the transducer to the seabed and back to the transducer. The second goes from the transducer to the seabed back to the sea surface (including part of the ship's hull), back to the seabed and finally back to the transducer. RoxAnn uses the energy in the tail of the first echo as a measure of sea floor roughness and the total energy in the second echo as a measure of sea floor "hardness". These two parameters are really indices of seabed acoustic backscatter and acoustic impedance, respectively.

The second most used commercial system is QTC-View, from Quester Tangent Corporation (QTC) [25,15]. QTC uses only the first echo, calculating 166 statistical parameters from it. Principal Component Analysis is used to derive three "Q-

factors", which are linear combinations of the 166 parameters. These three Q-factors are the three major Principal Components specifying the shape of the waveforms. The system then clusters seabed types in either a supervised or unsupervised classification mode, much like methods (i) and (ii) above, respectively.

It is important to better understand what these empirical seabed classification systems are really measuring, and to determine how well they can be expected to work. To these ends existing models of seabed acoustic backscatter are being utilised to examine the characteristics of acoustic returns from the seabed at steep grazing angles (e.g. 65° to 90°) for frequencies between 10 and 100 kHz [22]. A widely used model is that of Jackson [2], in which seabed backscatter is modelled as the sum of both a surface and a volume term. The model provides backscatter as a function of grazing angle, but no information on backscatter versus time, so that it provides no information about the shape of a return pulse. Examination of the model indicates that for the above range of grazing angles, and all but the very roughest of surfaces, the Kirchhoff approximation provides a good model of the surface scattering contribution. It can also be concluded, for realistic ranges of input parameters, that the dominant factors influencing backscatter are: roughness size; the ratio of sediment to water acoustic impedance; and a volume backscattering parameter,  $\sigma_v$ , the dimensionless backscattering cross section per unit solid angle per unit area due to volume scattering below the sediment surface.

It should be possible, from real data of acoustic backscatter versus grazing angle, to estimate these three parameters, because of their different influences on the shape of the backscatter versus grazing angle curve. From these three parameters it would then be possible to infer sediment type. Curves for typical sediments are shown in Figure 3. However echosounders obtain backscatter versus time over a range of grazing angles, not backscatter versus grazing angle.

To examine the time evolution of the return pulse from a seabed surface a model, called BORIS-3D (Bottom Response from Inhomogeneities and Surface) was recently developed at NATO's SACLANT Undersea Research Centre in La Spezia, Italy [24,3]. This model uses the Kirchhoff approximation for the surface scattering and Small Perturbation theory for volume scattering. For a given transmitted impulse shape, surface and volume backscattered time-series are computed and summed. Figure 4 shows the geometry of the set-up. Surface and volume responses will generally overlap in time. Modelling of responses from various realistic sea floors is currently in progress.

#### 5. VOLUME BACKSCATTER (M.V. Hall)

Volume backscattering from within the water column gives rise to reverberation at any frequency, but the results discussed here are confined to frequencies between 2 and 20 kHz ( $\lambda$  from 75 to 7.5 cm). At these frequencies the major scattering objects are fish swim bladders, which contain air. Many species of fish have a swim bladder, with general function to keep the fish neutrally buoyant. Large shallow water fish have muscles attached to their bladder, and use it as

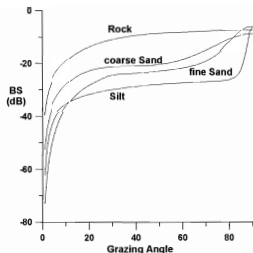


Figure 3. Modelled backscatter versus Grazing Angle Curves for different bottom types, using typical sediment parameters for each type. BS = Backscatter Strength.

wavelengths greater than the fish dimensions because it contains air. In addition there is also a low resonance frequency, which is determined by the elasticity of the air and the mass of the surrounding tissue and seawater.

### Simple bubble resonance theory

For a free spherical bubble of radius  $a$  in water of density  $\rho$ , the resonance frequency  $f_0$  is given by [21]:

$$f_0 = \sqrt{(3 \gamma P_0 / \rho)} / 2 \pi a \quad (4)$$

where  $\gamma$  is the ratio of specific heats, and  $P_0$  is the local hydrostatic pressure:  $P_0 = \rho g (z + 10)$ , in which  $z$  is depth in metres. For a radius of 2 mm for example, the resonance frequency at the surface ( $z = 0$ ) is 1.6 kHz ( $\lambda = 94$  cm), whereas at a depth of 500 m it would be 12 kHz ( $\lambda = 13$  cm). These wavelengths are much greater than the bubble size, so the scattering is omnidirectional. The resonance wavelength being orders of magnitude larger than the size of the object is an unusual phenomenon. For a conventional Helmholtz resonator such as the milk bottle, the elasticity and mass are both those of the internal fluid, and the resonance wavelength is comparable to its length. For a bubble however, the properties come from different media: the elasticity is that of the gas, while the mass is that of the water. For a bubble encased in solid tissue, the shear modulus also has an effect on the resonance frequency [1]. By modelling the bladder as a shell, the following approximate expression has been derived [11]:

$$f_0 = \sqrt{3 m \gamma P_0 / (4 \pi a^3 \rho / \phi - 4(m-1)d)} \quad (5)$$

where  $m$  is the ratio of the external to internal volumes of the shell ( $m = 2$ ),  $\phi$  is the shape correction factor to allow for the bladder being non-spherical ( $\phi \approx 1.1$ ), and  $d$  is the constant of proportionality in the relation between tissue shear modulus and frequency-squared ( $d = 0.001$  kg/m).

### Scattering cross-section

The scattering cross section ( $\sigma$ ) of an object is  $4\pi$  times its scattering or target strength, since  $\sigma$  gives the power scattered in all directions, while the scattering strength gives the power scattered per unit solid angle. At high frequencies ( $\lambda < a$ ) the scattering cross section approximately equals the cross-sectional area of the object ( $\sigma \approx \pi a^2$  for a sphere). At low frequencies the general behaviour is that  $\sigma \propto f^{-4}$  (Rayleigh scattering), and any resonance will appear as a perturbation. The scattering cross section at frequency  $f$  of an object resonant at frequency  $f_0$  is given by [5]:

$$\sigma(f) = 4 \pi a^2 / ((f_0/f)^2 - 1)^2 + \delta^2 \quad (6)$$

where  $\delta$  is the acoustic damping term. An expression for  $\delta$  for a free bubble was discussed by [8], and an adaptation to a swimbladder was given in [11]. In general its order of magnitude is 0.1.

At resonance the scattering cross section is

$$\sigma(f_0) = 4 \pi a^2 / \delta^2 \quad (7)$$

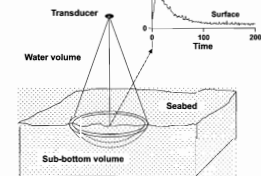


Figure 4. Construction of a simulated time series for reconstruction of bottom echoes. The echo starts on the first vertical contact of the ping with the seabed, and for subsequent sampling intervals is the sum of a surface contribution from annuli whose radii increase with time, coupled with volume contributions.

their vocal chord. Small deep-sea (mesopelagic) fish do not make sounds with it, but can pump dissolved air in, and back out, to maintain the bladder at a constant volume as they make diurnal depth migrations. Although only around 5% by volume of the fish body, the bladder dominates the scattering at all

As  $f/f_0 \rightarrow 0$ ,  $\alpha(f) \rightarrow 4\pi a^2 (f/f_0)^2$ . Equation (7) is not valid for high frequencies, since its derivation assumes the pressure to be uniform over the surface of the bubble, which is equivalent to assuming  $\lambda \gg a$ . As  $f/f_0 \rightarrow \infty$ , Eq. (6) yields  $\alpha(f) \rightarrow 4\pi a^2$  for small  $\delta$ , whereas the correct asymptote is  $\pi a^2$ .

#### Bio-mass estimates

Volume backscattering has been used by several institutions world-wide to estimate biomass. In Australasia the most active have been the New Zealand Ministry of Agriculture & Fisheries [9,7], and the CSIRO Division of Marine Research [10,18]. These surveys used narrow-band ultrasonic projectors as the sound source, and made use of the beam pattern of the emitted signal. A study involving one of the authors [12] used small explosive charges as the sound source. These are omnidirectional but contain useful energy over frequencies up to 20 kHz. Midwater trawls were conducted concurrently with an 8-square-metre net. The fish caught were weighed and sorted into classes based on mass. For each class the swimbladder size was estimated and the corresponding resonance frequency, for the known trawl depth, was determined using Eq. (6). From the population density of each class, the reverberation in each third-octave band from 2.5 to 20 kHz was computed using Eq. (7), and the results were compared with the measured reverberation. There was generally good agreement at frequencies above 8 kHz. The main difference was that although the trawls did not catch any fish heavier than 3 g, the acoustic results indicated that many heavier fish were in fact present. This difference was attributed to the ability of these larger fish to escape capture.

#### Effect on sonar

It is important for active sonars to have a narrow beam pattern, for both localising a target, and also to reduce the level of reverberation. Because of the large volumes of water ensonified by a sonar beam at long ranges, volume reverberation is generally the environmental parameter that limits the performance of long range active sonar. By having a database or model of the dependence of backscattering on frequency, geographic location, time of day, and depth, a sonar operator can adjust the carrier frequency of a sonar to obtain the optimum performance for a given location and time of day.

## 6. TURBIDITY (L.J. Hamilton)

Measurements of suspended sediment concentration (SSC) profiles in aquatic environments are used for diverse purposes e.g. examination of turbidity or water clarity, pollution studies, underwater visibility, sediment transport rates, and knowledge of the dynamics affecting turbidity e.g. wave processes. It is possible to estimate SSC at high temporal (0.1–1 s) and spatial (1–10 cm) resolutions with Acoustic Backscatter (ABS) instruments, and to remotely and non-intrusively monitor and image suspension processes in real-time. ABS instruments infer SSC profiles by emitting bursts of MHz frequency pulses, and time gating the return. Narrow beamwidths are used e.g. 1.5°. Ranges of 10–20 m may be obtained at 0.5 MHz, and about 1 m for 3 MHz. After allowance for transmission losses, and by making some simple assumptions about suspended sediment properties, the backscatter can be directly related to SSC.

The backscatter processes may be described by single scattering theory [30]. Negligible grain shielding and negligible multiple scattering are assumed, with allowance for near and far-field transducer beam patterns, beam spreading, and absorption due to water and the suspended sediment itself. Absorption by suspended sediment is assumed to be proportional to SSC, a simple assumption yielding good results [30]. Attenuation constant for a particular sediment particle size may be calculated from formulae [27,28], and absorption due to water is calculated from temperature and salinity measurements. The backscattered pressure or voltage signals received by the transducer from scatterers in a particular range bin are treated as incoherent [29] (also see Section 2), allowing them to be squared and summed without phase considerations.

If backscatter were sensitive to particle volume, then for constant particle density, changes in size distribution during measurements would not affect inferences of SSC [20]. However, in the Rayleigh region the size, shape, and density of irregularly shaped particles chiefly determine the backscatter [28,27]. To overcome this it is commonly assumed particle size distribution and particle backscatter function at a site are invariant during measurements, and that only total concentration varies at any depth in the column, a necessary but weak link in the calibration [20]. To reduce variability in the Rayleigh distributed backscatter from a particular range bin, backscatter values are averages for pulse trains. With the stated assumptions, backscatter is linearly proportional only to concentration, and SSC can be obtained to within 20–30%.

Calibration is usually performed after laboratory determinations of SSC have been obtained from water samples, but useful field calibrations can be made in conjunction with optical devices [13]. In the latest developments in this field, multifrequency devices are used to infer both SSC and particle diameter [19,31], although inversions are subject to noise, and only short ranges of about 1 metre are obtained. ABS instruments provide a highly versatile means of routinely obtaining information on dynamic turbidity events and suspension profiles.

## 7. CONCLUSION

Acoustical backscattering is an extremely useful means of probing the oceanic environment which finds application over a wide range of technology and physical processes. In usefulness and scope it may be compared to satellite based remote sensing techniques, although having a more limited scale, with both technologies being able to probe large areas in short times in a repeatable fashion. Other applications of acoustic backscatter employing very different principles than those discussed here also exist e.g. use of Doppler shift from scatterers to infer current profiles; characterisation of vegetation by classifying the jagged pattern obtained when transiting the vegetation; and estimates of fish populations by echo counting. From being merely a hindrance to sonar applications, backscatter is now a fully realized tool for diverse oceanic investigations.

## REFERENCES

1. I.B. Andreeva, Scattering of sound by air bladders of fish in deep sound-scattering layers (English translation). *Soviet Physics Acoustics* **10**, 17–20 (1964)
2. *Applied Physics Laboratory*, APL-UW High Frequency Ocean Environmental Acoustic Models Handbook, *Technical Report APL-UW TR-9407*, October 1994, *Applied Physics Laboratory, University of Washington, Seattle*.
3. O. Bergem, E. Pouliquen, G. Canepa and N.G. Pace, "Time-evolution modelling of seafloor scatter. II. Numerical and experimental evaluation", *J. Acoust. Soc. Am.* **105**, 3142–3150 (1999)
4. D.R. Burns, C.B. Queen, H. Sisk, W. Mullarkey and R.C. Chivers, Rapid and convenient acoustic sea-bed discrimination for fisheries applications". *Proceedings of the Institute of Acoustics* **II**, Part 3, 169–178 (1989)
5. E.L. Carstensen and L.L. Foldy, Propagation of sound through a liquid containing bubbles. *J. Acoust. Soc. Am.* **59**, 461–503 (1947)
6. S. Clay S. and H. Medwin, *Acoustical oceanography: principles and applications*. John Wiley and Sons. New York (1977)
7. R.F. Coombs and P.L. Cordue, Evolution of a stock assessment tool: acoustic surveys of spawning hoki (*Macruronus novaezelandiae*) off the west coast of South Island, New Zealand, 1985–91. *New Zealand Journal of Marine & Freshwater Research* **29**, 175–194 (1995)
8. C. Devin, Survey of thermal, radiation and viscous damping of pulsating air bubbles in water. *J. Acoust. Soc. Am.* **31**, 1654–1667 (1959)
9. M.A. Do and R.F. Coombs, Acoustic measurements of the population of Orange Roughy (*Hoplostethus atlanticus*) on the North Chatham Rise (N.Z.) in 1986. *New Zealand Journal of Marine & Freshwater Research* **23**, 225–237 (1989)
10. N.G. Elliott and R.J. Kloser, Use of acoustics to assess a small aggregation of orange roughy, *Hoplostethus atlanticus* (Collett), off the east coast of Tasmania. *Australian Journal of Marine & Freshwater Research* **44**, 473–482 (1993)
11. M. Hall, Measurements of acoustic volume backscattering in the Indian and Southern Oceans. *Australian Journal of Marine & Freshwater Research* **32**, 855–876 (1981)
12. M. Hall and A.F. Quill, Biological sound scattering in an ocean eddy. *Australian Journal of Marine & Freshwater Research* **34**, 563–572 (1983)
13. L.J. Hamilton, Calibration and interpretation of acoustic backscatter measurements of suspended sediment concentration profiles in Sydney Harbour. *Acoustics Australia* **26**(3), 87–93 (1998)
14. L.J. Hamilton, P.J. Mulhearn and R. Poekert, A Comparison Of RoxAnn And QTC-View Acoustic Bottom Classification System Performance For The Cairns Area, Great Barrier Reef, Australia. *Continental Shelf Research* **19**(12), 1577–1597 (1999)
15. [http://marine.questerlangent.com/n\\_sitemap.html](http://marine.questerlangent.com/n_sitemap.html)
16. <http://www.seabed.co.uk/NewFiles/ROXANN/hydropr.html>
17. R. Kloser, T. Koslow, T. Ryan, and P. Sakov, Species identification in deep water using multiple frequencies. Program and Abstracts, 13th National Congress of the Australian Institute of Physics (page 159) (1998)
18. R.J. Kloser, J.A. Koslow, and A. Williams, Acoustic assessment of a spawning aggregation of Orange Roughy (*Hoplostethus atlanticus*, Collett) off South-eastern Australia, 1990–93. *Marine & Freshwater Research* **47**, 1015–1024 (1996)
19. T. H. Lee and D.M. Hanes, Direct inversion method to measure the concentration profile of suspended particles using backscattered sound. *J. Geophysical Research* **100**, C2, 2649–2657
20. C. Libicki, K.W. Bedford and J.F. Lynch, The interpretation and evaluation of a 3-MHz acoustic backscatter device for measuring benthic boundary layer sediment dynamics. *J. Acoust. Soc. Am.* **85**(4), 1501–1511 (1989)
21. M. Minnaert, On musical air-bubbles and the sounds of running water. *Philosophical Magazine* **16**, 235–248 (1933)
22. P. J. Mulhearn, Modelling Acoustic Backscatter from Near-Normal Incidence Echosounders — Sensitivity Analysis of the Jackson Model, *DSTO Technical Note DSTO-TN-0304*, September 2000
23. P.D. Osborne, C.E. Vincent and B. Greenwood, Measurements of suspended sand concentrations in the nearshore: field intercomparison of optical and acoustic backscatter sensors. *Continental Shelf Research* **14**, 159–174 (1994)
24. E. Pouliquen, O. Bergem and N.G. Pace, Time-evolution modelling of seafloor scatter. I. Concept, *J. Acoust. Soc. Am.* **105**, 3136–3141 (1999)
25. B.T. Prager, D.A. Caughey and R.H. Poekert, "Bottom classification: operational results from QTC View" *OCEANS '95 — Challenges of Our Changing Global Environment Conference*, San Diego, CA, USA, October 1995
26. M. Readhead, Acoustic daylight — using ambient noise to see underwater, *Acoustics Australia* **29**(2), 63–68 (2001)
27. A.S. Schaafsma and A.E. Hay, Attenuation in suspensions of irregularly shaped sediment particles: A two-parameter equivalent spherical scatterer model. *J. Acoust. Soc. Am.* **102**(3), 1485–1502 (1997)
28. J. Sheng J. and A.E. Hay, An examination of the spherical scatterer approximation in aqueous suspensions of sand. *J. Acoust. Soc. Am.* **83**(2), 598–610 (1988)
29. P.D. Thorne and P.J. Hardcastle, Acoustic measurements of suspended sediments in turbulent currents and comparison with in-situ samples. *J. Acoust. Soc. Am.* **101**(5), Pt 1, 2603–2614 (1997)
30. P.D. Thorne, C.E. Vincent, P.J. Hardcastle, S. Rehman and N. Pearson, Measuring suspended sediment concentration using acoustic backscatter devices. *Marine Geology* **98**, 7–16 (1991)
31. E.D. Thosteson and D.M. Hanes, A simplified method for determining sediment size and concentration from multiple frequency acoustic backscatter measurements. *J. Acoust. Soc. Am.* **104**(2), Pt 1, 820–830.